problems of nonlinear filtration," in: Proceedings of a Seminar on Boundary Problems [in Russian], No. 11, Izd. Kazansk. Univ., Kazan' (1974), pp. 25-31.
18. E. G. Sheshukov, "Behavior of the solutions of problems of nonlinear filtration in the vicinity of the line of degeneration of the region of the velocity hodograph," Izv. Vyssh. Uchebn. Zaved., Mat., No. 4, 114-119 (1974).

PLANE WAVES IN NONLINEAR VISCOUS MULTICOMPONENT MEDIA

G. M. Lyakhov and V. N. Okhitin

UDC 624.131+532.529

Wave processes in multicomponent media (liquid and water-saturated soil with bubbles of gas, suspensions, etc.) have been studied in [1-20] and other investigations.

In [1] it was assumed that the space is filled with a number of continuous media, each of which corresponds to a component of the medium. The investigation was concerned with interpenetrating motions of these media (in the general case each moves with its own velocity and pressure). In the model of [2] the multicomponent medium was regarded as a homogeneous continuous medium with a compressibility equation taking account of the compressibility and the presence of components that were in an equilibrium state. In [3] the multicomponent medium was regarded as homogeneous, and the compressibility of the gaseous component was determined by Hugoniot's adiabatic curve. The reflection of a plane wave from a solid partition for various angles of incidence was investigated in [4] on the basis of [2], using electronic computers. The problem of the propagation of a wave produced by the explosion of the spherical charge of a blast wave, using the model of [2] as a basis, was solved by means of electronic computers in [5]. The authors of [6] proposed a model of a homogeneous medium analogous to that of [2] and obtained solutions of problems concerning the passage of a wave through a layer of water with gas bubbles and the reflection of the wave from a fixed boundary. The special characteristics of the structure of waves in water with gas bubbles and the effect of viscosity dissipation related to the motion of the bubbles with respect to the liquid were considered in [7]. In the model of [8] the pulsation of the bubbles was assumed to conform to Lamb's equation, i.e., the lack of equilibrium between the phases was taken into consideration. The case of strong shock waves, on the basis of [8], was considered in [9]. In [10, 11] it was shown that in a liquid with gas bubbles, for specific relationships between the viscosity, the load, and the bubble radius, there is formed a wave with an oscillator structure. In [12] the structure of a wave was investigated on the basis of the model of [13], with oscillations taken into consideration. Equations for the mechanics of a two-velocity two-temperature medium with two pressures were proposed in [14]. In [15], on the basis of [14], the structure of a stationary wave was investigated with thermal conductivity taken into account. It was shown that the nature of the pulsation depends substantially on the heat exchange between the phases. It was noted that the experiments of [11] should be analyzed with the time-dependent change of structure taken into account. In the experiments of [16] it was established that an increase in the intensity of the wave leads to an increase in the frequency and amplitude of the oscillations on the front, while an increase in the bubble diameter leads to a decrease of the frequency and an increase of the amplitude. Weak waves were considered. The authors of [17] obtained numerical solutions making it possible to determine the amplitude oscillations on the wave front, the velocity of propagation of the wave, and the time required for establishing a stationary structure. Waves in water-saturated rocks were considered in [18]. The authors of [18] obtained an equation describing weak longitudinal waves with inertial relaxation taken into account. The effect of the tension surface was investigated in [19]. In [20] the model of [2] was improved by the introduction of nonlinear diagrams for the dynamic and static compression of the multicomponent medium, making it possible to introduce bulk viscosity. The effect of viscosity was considered in a somewhat different manner in [21].

Moscow. Translated from Zhurnal Prikladnoi Mekhaniki i Tekhnicheskoi Fiziki, No. 2, pp. 121-130, March-April, 1977. Original article submitted April 22, 1976.

In what follows, using [20] as a basis, we obtain a solution of the problem of the propagation of a plane wave produced by a shock-type stationary load in a multicomponent medium. The solution was carried out on an electronic computer by the method of characteristics applied to viscosity-free media [5, 20, 22] and also by an approximate analytic method.

1. Model of the Medium, Method of Numerical Solution. We shall use the model of [20]. At the initial (atmospheric) pressure α_1, α_2, and α_3 are the relative fractions by volume of the gaseous, liquid, and solid components; V_{10}, V_{20}, and V_{30} are the specific volumes; ρ_{10}, ρ_{20}, and ρ_{30} are the densities; c_{10}, c_{20}, and c_{30} represent the speed of sound in each; ρ_0 is the density of the medium; V_0 is the specific volume

$$\rho_0 = 1/V_0 = \alpha_1\rho_{10} + \alpha_2\rho_{20} + \alpha_3\rho_{30}, \quad \alpha_1 + \alpha_2 + \alpha_3 = 1.$$

At pressure p the volume, the density, and the speed of sound are V_1, V_2, V_3, ρ_1, ρ_2, ρ_3, c_1, c_2, c_3, respectively, the density of the medium is ρ, and its specific volume is V.

We assume that in the free state the components are compressed according to the equations

$$\begin{aligned} p &= p_0(\rho_1/\rho_{10})^{\gamma_1} \text{ gaseous:} \\ p &= p_0 + \frac{\rho_{20}c_{20}^2}{\gamma_2}\left[\left(\frac{\rho_2}{\rho_{20}}\right)^{\gamma_2} - 1\right] \text{ liquid:} \\ p &= p_0 + \frac{\rho_{30}c_{30}^2}{\gamma_3}\left[\left(\frac{\rho_3}{\rho_{30}}\right)^{\gamma_3} - 1\right] \text{ solid.} \end{aligned} \tag{1.1}$$

The first equation in (1.1) reduces to the form of Tait's equation. Therefore, for all the components

$$p = p_0 + \frac{\rho_{i0}c_{i0}^2}{\gamma_i}\left[\left(\frac{V_{i0}}{V_i}\right)^{\gamma_i} - 1\right], \; i = 1, 2, 3, \; p_0 = \frac{\rho_{10}c_{10}^2}{\gamma_1}. \tag{1.2}$$

The gaseous component is present in the form of fine bubbles. As the wave passes through, the compression of the gas bubbles, which are isolated from one another by the other components, takes place not instantaneously, but over a finite time, while the other components move in to fill the volume originally occupied by the bubbles. Therefore, in accordance with [20], we assume that instead of (1.2), the equation governing the compression of the gas in the medium is

$$p = p_0 + \frac{\rho_{10}c_{10}^2}{\gamma_1}\left[\left(\frac{V_1}{V_{10}}\right)^{-\gamma_1} - 1\right] - \eta\frac{\dot{V}_1}{V_{10}}, \tag{1.3}$$

where η is the coefficient of bulk viscosity of the medium.

The other components are compressed in accordance with the same equations as in the free state.

The equation of compressibility of a three-component medium, under these assumptions, takes the form

$$\frac{\dot{V}}{V_0} = \varphi(p)\,\dot{p} - \frac{\alpha_1}{\eta}\psi(p, V), \tag{1.4}$$

where

$$\varphi(p) = -\sum_{i=2}^{3}\frac{\alpha_i}{\rho_{i0}c_{i0}^2}\left[\frac{\gamma_i(p-p_0)}{\rho_{i0}c_{i0}^2} + 1\right]^{-(1+\gamma_i)/\gamma_i};$$

$$\psi(p, V) = p - p_0\alpha_1^{\gamma_1}\left\{\frac{V}{V_0} - \sum_{i=2}^{3}\left[\frac{\gamma_i(p-p_0)}{\rho_{i0}c_{i0}^2} + 1\right]^{-1/\gamma_i}\right\}^{-\gamma_i}.$$

As $\dot{V} \to \infty$ and $\dot{p} \to \infty$, we obtain from (1.4) the equation of dynamic compressibility of the medium:

$$\frac{V_D}{V_0} = \alpha_1 + \sum_{i=2}^{3}\alpha_i\left[\frac{\gamma_i(p-p_0)}{\rho_{i0}c_{i0}^2} + 1\right]^{-1/\gamma_i}, \; \varphi(p) = \rho_0\frac{dV}{dp}. \tag{1.5}$$

As $\dot{V} \to 0$ and $\dot{p} \to 0$, we obtain the equation of static compressibility of the medium:

$$\frac{V_s}{V_0} = \sum_{i=1}^{3}\alpha_i\left[\frac{\gamma_i(p-p_0)}{\rho_{i0}c_{i0}^2} + 1\right]^{-1/\gamma_i}. \tag{1.6}$$

The last equation coincides with the equation of compressibility of the model of [2], not taking account of bulk viscosity. The model of [2] corresponds to the limiting equilibrium state of the medium, which corresponds to static compression in the model of [20].

We make use of Lagrange's variables: r is the space coordinate, t is the time.

We find the parameters of the wave produced by a load specified at the initial cross section r = 0 of the half-space (or a tube filled with the medium), increasing at t = 0 by a jump to p_S and retaining this value thereafter.

The fundamental equations of motion take the form

$$\frac{\partial u}{\partial r} - \rho_0 \frac{\partial V}{\partial t} = 0, \quad \frac{\partial u}{\partial t} + \frac{1}{\rho_0}\frac{\partial p}{\partial r} = 0. \tag{1.7}$$

The system (1.7), closing (1.4), is of hyperbolic type. The characteristic relations are

$$dp \pm \left(\frac{\rho_0}{\varphi(p)}\right)^{1/2} du = \frac{\alpha_1 \psi(p, V)}{\eta \varphi(p)} dt \quad \text{for} \quad \dot{r} = \pm(-\rho_0 \varphi(p))^{-1/2};$$
$$dp - \frac{\rho_0}{\varphi(p)} dV = \frac{\alpha_1 \psi(p, V)}{\eta \varphi(p)} dt \quad \text{for} \quad r = 0. \tag{1.8}$$

The characteristics of the first and second families are nonlinear.

The boundary conditions at the initial cross section r = 0 and at the jump (the shock front), where the compression takes place according to the dynamic diagram and there is no viscosity, have the form

$$p = p_0 \text{ for } t \leqslant 0, \; p = p_S \text{ for } t \geqslant 0,$$
$$p - p_0 = \rho_0 u D, \; (\rho - \rho_0) D = \rho u.$$

The solution was carried out on the BÉSM-6 electronic computer for three load values $p_S/p_0 = 5000$, 1000, and 50, and for six media, whose characteristics are given in Table 1 [1-3) water-saturated soil; 4-6) water with air bubbles].

In the calculations we assumed $\rho_{10} = 1.29$, $\rho_{20} = 10^3$, $\rho_{30} = 2.65 \cdot 10^3$ kg/m^3, $c_{10} = 330$, $c_{20} = 1500$, $c_{30} = 5000$ m/sec, $\gamma_1 = 1.4$, $\gamma_2 = 7$, $\gamma_3 = 4$.

In the problem under consideration, in the r–t plane we have four types of points, at each of which the parameters are calculated according to their appropriate algorithms: at the shock front, in regions of increasing and constant pressure, and at the initial cross section.

We consider the sequence of calculation of the parameters in the region of increasing pressure. Suppose that points A, B, D lie in the same time layer and that the parameters at these points are known, r(A) < r(B) < r(D). We determine the parameters at point C, which lies in the next time layer and has the same space coordinate as point B. The time step Δt varies from layer to layer. From point C on the preceding time layer we draw the characteristics of all three families. Their intersections with the curve AD will be denoted by L, B, M. The coordinates of points L and M are found from the equations

$$r_L = r_C - [-\rho_0 \varphi(p)]_{CL}^{-1/2} \Delta t, \quad r_M = r_C + [-\rho \varphi(p)]_{CM}^{-1/2} \Delta t.$$

The subscript CL indicates that the quantities in brackets are taken as the average of their values at points C and L. In the first calculation the parameters at point C are taken to be the same as at point B. Using interpolation with respect to the values of the parameters at points A, B, and D, we calculate the values of p, V, and u at points L and M. After this, using the values we have found, we find more exact values for p, u, and V at point C:

$$p_C - p_L = -[-\rho_0/\varphi(p)]_{CL}^{1/2}(u_C - u_L) - \frac{\alpha_1}{\eta}\left(\frac{\psi(p, V)}{\varphi(p)}\right)_{CL} \Delta t,$$
$$p_C - p_M = \left[-\frac{\rho_0}{\varphi(p)}\right]_{CM}^{1/2}(u_C - u_M) - \frac{\alpha_1}{\eta}\left(\frac{\psi(p, V)}{\varphi(p)}\right)_{CL} \Delta t,$$
$$p_C - p_B = -\left(\frac{\rho_0}{\varphi(p)}\right)_{CB}(V_C - V_B) - \frac{\alpha_1}{\eta}\left(\frac{\psi(p, V)}{\varphi(p)}\right)_{CB} \Delta t.$$

The equations correspond to the relations satisfied along the three characteristics. The calculation is repeated a prescribed number of times. The calculation of the parameters at other types of points is carried out in the same way.

TABLE 1

Number of medium	α_1	α_2	α_3
1	0,01	0,39	0,6
2	0,02	0,38	0,6
3	0,04	0,36	0,6
4	0,01	0,99	0
5	0,04	0,96	0
6	0,10	0,90	0

TABLE 2

Number of medium	$A \cdot 10^{-6}$, kg/m^2 · sec	p_S^*/p_0	$\eta \cdot 10^{-3}$, kg/m · sec
1	3,28	1850	1,09
2	3,34	3000	1,11
3	3,39	4750	1,13
4	1,52	1250	0,51
5	1,53	2930	0,52
6	1,58	5420	0,53

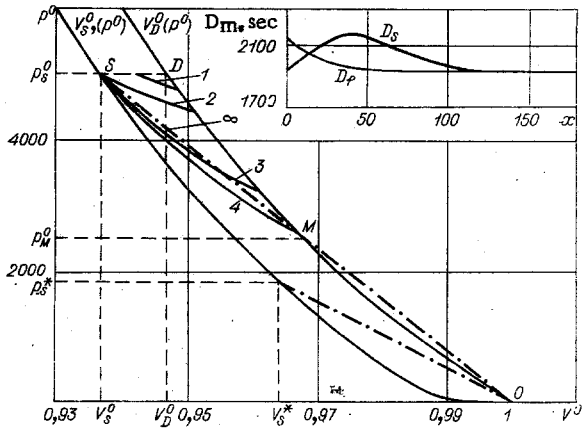

Fig. 1

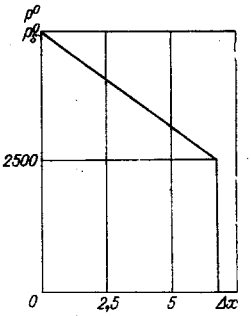

Fig. 2

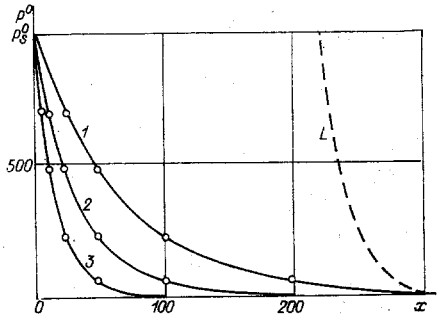

Fig. 3

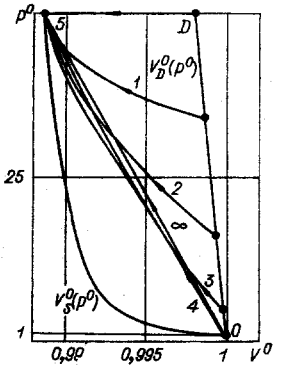

Fig. 4

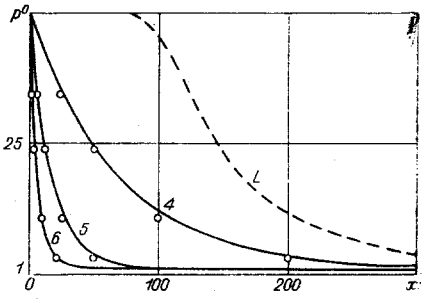

Fig. 5

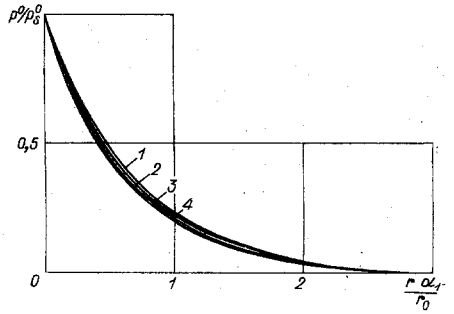

Fig. 6

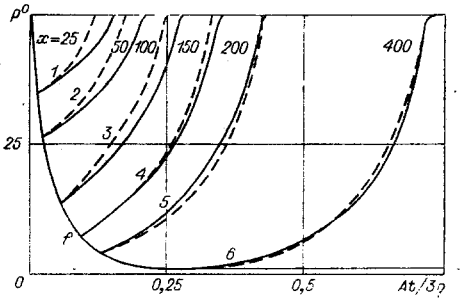

Fig. 7

2. Results of the Numerical Solution. Figure 1 shows the diagrams of the dynamic compression $V_D^0(p^0)$ and the static compression $V_S^0(p^0)$ of medium 1 (see Table 1), constructed in accordance with Eqs. (1.5), (1.6). Here and hereafter, $p^0=p/p_0$, $V^0=V/V_0$. For small pressures, when the compressibility of the medium is determined by the compressibility of the air, the curves differ from each other considerably. Starting with pressures of the order of tens of atmospheres, the air is compressed to a state close to the limiting state and the curves become similar to each other; the $V_S^0(p^0)$ diagram differs from the $V_D^0(p^0)$ diagram by α_1.

The calculations show that at time $t=0$, when the load is applied, the shock front begins to advance from the cross section $r=0$. The initial pressure at the shock front is $p_S^0=5\cdot 10^3$, and its velocity is $D_f=[(p_S^0-1)p_0/\rho_0(1-V_D^0)]^{1/2}$. The value of the jump at the shock front and its velocity decrease with distance. Behind the jump there follows a region of gradual increase of pressure to p_S^0.

As time increases, the state at the shock front along the $V_D^0(p^0)$ curve passes from point D to point M, and at the initial cross section from point D to point S. In the region of increasing pressure the state is determined by curves $1-\infty$. The increasing numbers correspond to increasing time. Curve 2 relates to the instant of time at which the state at the initial cross section reaches the static-compression diagram. From the initial cross section the front of the region of constant pressure p_S^0 begins to propagate itself with velocity $D_S<D_f$. With increasing time, D_f decreases while D_S first increases and then decreases (see Fig. 1). As $t\to\infty$, the diagram of state in the region of increasing pressure approaches the straight line OMS, the pressure at the shock front approaches p_M^0, and the velocity of the shock front and the front of the region of constant pressure and the states between them approaches D_M (the flow becomes stationary)

$$D_M=[(p_M^0-1)\,p_0/\rho_0\,(1-V_M^0)]^{1/2}.$$

We introduce the dimensionless distance

$$x=Ar/3\eta; \tag{2.1}$$

$$A=\left(\frac{\alpha_2\rho_{20}+\alpha_3\rho_{30}}{1-\alpha_1}\right)^{1/2}\left(\frac{\alpha_2}{\rho_{20}c_{20}^2}+\frac{\alpha_3}{\rho_{30}c_{30}^2}\right)^{-1/2}. \tag{2.2}$$

(A is the acoustic resistance of the medium surrounding the gas bubbles). The values of A calculated according to (2.2) are shown in Table 2. Neglecting the mass of the air in comparison with the mass of the other components, we obtain for small values of α_1

$$A=\rho_0^{1/2}\left(\frac{\alpha_2}{\rho_{20}c_{20}^2}+\frac{\alpha_3}{\rho_{30}c_{30}^2}\right)^{-1/2}.$$

Figure 2 shows the distribution of the pressure for medium 1 when $p_S^0=5000$. The variation of $p^0(x)$ is nearly linear. The length of the region of increasing pressure is $\Delta x=6.8$, $p_M^0\cong p_S^0/2$. Assuming, in accordance with [20], that $\eta=1.09\cdot 10^3$ kg/m·sec, we obtain the dimensional length of the region of increasing pressure, $\Delta r=6.8\cdot 10^{-3}$ m, and the time of the increase at a fixed point of the medium, $\Delta t=3.5\cdot 10^{-6}$ sec. The time of the increase is quite short.

The case we have considered, when the jump at the shock front decreases to a finite value, arises only at a fairly large load, $p_S^0>p_S^*$. If the straight line OS (see Fig. 1) does not intersect the dynamic diagram at even one point, then the value of the jump at the shock front approaches zero in the limiting case; p_S^* is found from the condition

$$p_S^*-1=-c_0^2\rho_0(V_S^*-1),\quad V_S^*=V_S^0(p_S^*); \tag{2.3}$$

$$c_0^2\rho_0=\left(\frac{\alpha_2}{\rho_{20}c_{20}^2}+\frac{\alpha_3}{\rho_{30}c_{30}^2}\right)^{-1},\quad c_0\rho_0\approx A. \tag{2.4}$$

The values of p_S^* calculated in accordance with (2.3), (2.4) are shown in Table 2.

As the percentage of the gaseous component increases, so does p_S^*. In a water–air medium p_S^* is less than in a water-saturated soil for the same value of α_1. The velocity of the shock front approaches the velocity of sound c_0. For the first medium $c_0=1640$ m/sec.

The variation of the pressure at the shock front as a function of the distance in water-saturated soils for $p_S^0=1000<p_S^*$ is shown in Fig. 3, where the numbering of the curves corresponds to the numbering of the media in Table 1.

Curve L defines the distribution of pressure in medium 1 when the shock front reaches the point x=303. The pressure at the shock front is practically equal to zero. The length of the region of increasing pressure is $\Delta x=83$. For $\eta=1.09\cdot 10^3$ kg/m·sec we obtain $r=30.3\cdot 10^{-2}$ m, $\Delta r=8.3\cdot 10^{-2}$ m. The time of increase of the pressure to the maximum, $\Delta t=5\cdot 10^{-5}$ sec, is still small. As p_S^0 decreases, the length of the region of increasing pressure increases. As the percentage of the gaseous component increases, so does the intensity of extinction at the shock front.

Figure 4 shows the diagrams for the dynamic compression $V_D^0(p^0)$ and static compression $V_S^0(p^0)$ of water with gas bubbles (medium 4); curves $1-\infty$ define the variation of the state in the particles of the medium as the pressure increases. The numbering increases with the distance of the particles from the initial cross section. The curves approach the straight line OS.

Figure 5 shows how pressure at the shock front varies with the distance in a water–air medium for $p_S^0=50$. The numbering of the curves corresponds to the numbering of the media in Table 1. The pressure at the shock front approaches zero. Curve L defines the distribution of pressure in medium 4 when the shock front reaches x=398.

3. Approximate Values of the Coefficient of Viscosity. The solutions of wave problems [20] have shown that the bulk viscosity leads to a blurring of the shock wave. The values of the coefficient of bulk viscosity η must be determined experimentally. Let us find the approximate values of η from an analysis of the compression of the bubbles, taking the equations of compressibility of the solid and liquid components to be linear. Suppose that all the bubbles are spherical in shape and have the same radius r_0. The initial volume of a bubble is $V_0^*=4\pi r_0^3/3$. For compression at the time the load is applied,

$$\dot{V}^* = -4\pi r_0^2 u,$$

where u is the velocity of the medium surrounding the bubbles. The variation of the volume of all the bubbles in a unit volume of the medium is given by

$$\frac{\dot{V}_1}{V_{10}} = \frac{\dot{V}^*}{V_0^*} = -\frac{4\pi r_0^2 u}{V_0^*} = -\frac{3u}{r_0}.$$

From (1.3) it follows that at this instant of time

$$p - p_0 = -\eta \dot{V}_1/V_{10} = 3\eta u/r_0. \tag{3.1}$$

If the solid and liquid components are linear-elastic media, i.e., $\gamma_2=\gamma_3=-1$, then

$$p - p_0 = Au,\ A = \left(\frac{\alpha_2\rho_{20}+\alpha_3\rho_{30}}{1-\alpha_1}\right)^{1/2}\left(\frac{\alpha_2}{\rho_{20}c_{20}^2}+\frac{\alpha_3}{\rho_{30}c_{30}^2}\right)^{-1/2}. \tag{3.2}$$

From a comparison of (3.1), (3.2) we find the coefficient of viscosity

$$\eta = Ar_0/3. \tag{3.3}$$

The values of η for $r_0=10^{-3}$ m, calculated according to (3.3), are shown in Table 2. For the types of variation of α_1 we have considered, the values of A and η vary only slightly.

In water-saturated soil A and η are higher than in a water–air medium for the same air content and the same bubble radii.

Variation of the gaseous-component leads to a variation in the static and dynamic diagrams, while variation of the bubble radius changes the coefficient of viscosity of the medium.

From (2.1), (3.3) it follows that

$$x = r/r_0.$$

In Fig. 6, curves 1-4 define the pressure at the shock front for $p_S^0=50$, 500, 1000, and 3000, respectively. They were constructed for water-saturated soil, but they practically coincide with the curves for water with air bubbles. The difference between the curves is no more than 10%. From this it follows that when $p_S^0 < p_S^*$, we can assume as a first approximation that

$$p^0/p_S^0 = f(r\alpha_1/r_0).$$

4. Analytic Solutions. We consider the case $p_S^0 < p_S^*$. We approximate the dynamic-compression diagram by the straight line OD (see Fig. 4). In the linearization the characteristics are straight lines, the curve of the front coincides with the characteristic of the first family, and the parameters at the shock front correspond to the first equation in (1.8). The function $\psi(p, V)$ can be represented in the form

$$\psi(p, V) = p - p_0[1 - (V_D^0 - V^0)/\alpha_1]^{-\gamma_1}. \tag{4.1}$$

As $V^0 \to V_D^0$ and $V^0 \to V_S^0$, respectively, we have $\psi \to p - p_0$ and $\psi \to 0$. On the dynamic-compression diagram, and consequently at the jump as well, we have $\psi = p - p_0 = p_0(p^0 - 1)$. In accordance with (1.5), for the linearization we obtain

$$\varphi(p) = \rho_0 dV/dp, \quad \varphi(p) = (1 - V_D^0)/p_0(1 - p_S^0) = \text{const}.$$

The relation at the jump is

$$p = (-dp/dV)^{1/2}u = (-\rho_0/\varphi(p))^{1/2}u.$$

Hence the first equation in (1.8) takes the form

$$dp^0/(p^0 - 1) = -\alpha_1 p_0(p_S^0 - 1)/\eta(1 - V_D^0)\,dt.$$

Integrating for the initial condition $p_S^0 = p^0(0)$, we obtain the variation of the pressure at the shock front as a function of time:

$$\ln[(p^0 - 1)/(p_S^0 - 1)] = -\alpha_1 p_0(p_S^0 - 1)\,t/2\eta(1 - V_D^0).$$

The equation of motion of the shock front is

$$r = [p_0(p_S^0 - 1)/(1 - V_D^0)\rho_0]^{1/2}t.$$

The variation of the pressure at the shock front as a function of distance is given by

$$\ln[(p^0 - 1)(p_S^0 - 1)] = -\alpha_1[(p_S^0 - 1)\,p_0\rho_0]^{1/2}\,r/2\eta(1 - V_D^0)^{1/2}. \tag{4.2}$$

In Fig. 3 and Fig. 5 the indicated points correspond to the pressure at the shock front as calculated according to (4.2). The analytic solution for the linearization of the dynamic-compression diagram is close to the solution obtained by electronic computer without linearization (curves 1-6). The reason for this is that the dynamic-compression diagram deviates little from a linear function (see Figs. 1 and 4) in the media under consideration.

We consider the variation of the pressure at a fixed point of the medium when $p_S^0 < p_S^*$. For $\dot{r} = 0$ the third equation in (1.8) is satisfied. After the jump at the shock front up to p_f^0 the state at a particle changes according to curves $1 - \infty$ (see Fig. 4). For linearization of these curves and of the dynamic-compression diagram we obtain

$$\frac{dV}{dp} = \frac{V_S^0 - V_f^0}{(p_S^0 - p_f^0)\,p_0\rho_0}, \quad \varphi(p) = -\frac{1 - V_D^0}{p_0(p_S^0 - 1)}, \tag{4.3}$$

where p_f^0 is the pressure at the jump; $V_S^0 = V_S^0(p_S^0)$; $V_D^0 = V_D^0(p_S^0)$.

Between the dynamic and static diagrams, except for a small region near the static curve, we can approximately assume [see (4.1)] the condition $\psi = p - p_0$. From this, taking account of (4.3), we obtain the third equation in (1.8) in the form

$$dp^0/(p^0 - 1) = \alpha_1(p_S^0 - p_f^0)\,p_0/\eta(V_S^0 - V_D^0)\,dt.$$

Integrating, we find the variation of the pressure at a fixed point of the medium (a particle) behind the shock front

$$\ln[(p^0 - 1)(p_f^0 - 1)] = \alpha_1(p_S^0 - p_f^0)\,p_0/\eta(V_S^0 - V_D^0)(t - t_f) \tag{4.4}$$

(t_f is the time when the shock front arrives at the point under consideration).

The time during which the pressure increases to p_S^0 is

$$\Delta t = \ln[(p_S^0 - 1)/(p_f^0 - 1)]\,\eta(V_S^0 - V_D^0)/\alpha_1(p_S^0 - p_f^0).$$

For values of p_S^0 that are not too small, we may assume $\alpha_1 = V_S^0 - V_D^0$.

In Fig. 7, curve f corresponds to the variation of pressure at the shock front with time in water with gas bubbles when $\alpha_1 = 0.01$ and $p_S^0 = 50$. Curves 1-6 show the variation of pressure at fixed points of the medium at distances x=25, 50, 100, 150, 200, and 400, respectively. The solid curves are obtained by computer calculations, while the dashed curves are obtained by (4.4). The differences between them are slight.

The analytic expressions obtained can be used for the approximate determination of the pressure at the shock front and its variation during the time the pressure increases to p_S^0, as well as for determining the time of pressure increase.

LITERATURE CITED

1. Kh. A. Rakhmatulin, "Fundamentals of the gasdynamics of interpenetrating motions of compressible media," Prikl. Mat. Mekh., 20, No. 27 (1956).
2. G. M. Lyakhov, "Shock waves in multicomponent media," Izv. Akad. Nauk SSSR, Mekh. Mashinostr. No. 1 (1959).
3. Kh. A. Rakhmatulin, "Propagation of waves in multicomponent media," Prikl. Mat. Mekh., 33, No. 4 (1969).
4. Z. Legowski and E. Wlodaczyk, "Regular reflection of an oblique stationary shock wave from an indeformable plane partition in saturated soil," Proc. Vibr. Probl., 15, No. 2 (1974).
5. G. M. Lyakhov and V. N. Okhitin, "Spherical blast waves in multicomponent media," Zh. Prikl. Mekh. Tekh. Fiz., No. 2 (1974).
6. B. R. Parkin, F. R. Gilmore, and G. L. Broad, "Shock waves in water with air bubbles," in: Underwater and Underground Explosions [Russian translation], Mir, Moscow (1974).
7. G. K. Batchelor, "Compression waves in suspensions of gas bubbles," in: Mekhanika [Periodic Collection of Translations of Foreign Articles], No. 3 (1968).
8. S. V. Iordanskii, "Equations of motion of a liquid containing gas bubbles," Zh. Prikl. Mekh. Tekh. Fiz., No. 3 (1960).
9. V. K. Kedrinskii, "Propagation of disturbances in a liquid containing gas bubbles," Zh. Prikl. Mekh. Tekh. Fiz., No. 4 (1968).
10. V. E. Nakoryakov, V. V. Sobolev, and I. R. Shreiber, "Long-wave disturbances in a gas–liquid mixture," Izv. Akad. Nauk SSSR, Mekh. Zhidk. Gaza, No. 5 (1972).
11. L. Noordzij, "Shock waves in bubble-liquid mixtures," Phys. Commun., 3, No. 1 (1971).
12. L. Van Wijngaarden, "On the structure of shock waves in liquid–bubble mixtures," Appl. Sci. Res., 22, No. 5 (1970).
13. L. Van Wijngaarden, "On equations of motion for mixtures of fluid and gas bubbles," J. Fluid Mech., 33, No. 3 (1968).
14. R. I. Nigmatulin, "Small-scale flows and surface effects in the hydromechanics of multicomponent media," Prikl. Mat. Mekh., 35 (1971).
15. R. I. Nigmatulin, N. S. Khabeev, and V. Sh. Shagapov, "Shock waves in a liquid with gas bubbles," Dokl. Akad. Nauk SSSR, 214, No. 4 (1974).
16. S. S. Kutateladze, A. P. Burdukov, V. V. Kuznetsov, V. E. Nakoryakov, B. G. Pokusaev, and I. R. Shreiber, "The structure of a weak shock wave in a gas–liquid medium," Dokl. Akad. Nauk SSSR, 207, No. 2 (1972).
17. S. S. Kutateladze, V. E. Nakoryakov, V. V. Sobolev, and I. R. Shreiber, "Dynamics of shock waves in a liquid containing gas bubbles," Zh. Prikl. Mekh. Tekh. Fiz., No. 5 (1974).
18. V. N. Nikolaevskii, K. S. Basniev, A. G. Gorbunov, and G. A. Zotov, Mechanics of Saturated Porous Media [in Russian], Nedra, Moscow (1970).
19. G. F. Kopytov, "Attenuation of shock waves in a gas–liquid medium," Vestn. Leningr. Univ., No. 1 (1968).
20. G. M. Lyakhov, Fundamentals of the Dynamics of Blast Waves in Soils and Rocks [in Russian], Nedra, Moscow (1974).
21. E. A. Koshelev, "Development of a camouflet cavity as a result of explosion in soft ground," Zh. Prikl. Mekh. Tekh. Fiz., No. 2 (1975).
22. N. E. Hoskin, "The method of characteristics for the solution of the equations of one-dimensional nonstationary flow," in: Computational Methods in Hydrodynamics [Russian translation], Mir, Moscow (1967).